Z_{eff}-PROFILES IN DIFFERENT CONFINEMENT- AND HEATING REGIMES OF ASDEX

K.-H. Steuer, H. Röhr, D.E. Roberts*, A. Eberhagen, G. Janeschitz, G. Fußmann, O. Gruber, K. McCormick, H. Murmann, J. Roth, F. Wagner
*Atomic Energy Corp., Pretoria, RSA

Max-Planck-Institut für Plasmaphysik
EURATOM Association, Garching, FRG

Introduction

Z_{eff} is an important quantity in fusion research. It should ideally be as small as possible to minimize both fuel dilution and radiation losses. Further, radial profiles of Z_{eff}, together with $T_e(r)$, are needed to derive $j(r)$ used in stability analysis. We report measurements of Z_{eff} profiles for a variety of ASDEX plasmas: ohmic (H and D; gas and pellet fuelling), and co and counter neutral beam heated plasmas.

Z_{eff} measurements

Z_{eff} profiles are measured from the intensity of plasma radiation in the near infrared. In this wavelength region recombination and line radiation are generally unimportant and the radiation is mainly bremsstrahlung. The intensity profiles are measured with the ASDEX 16 channel YAG laser Thomson scattering system (Fig. 1) /Ref. 1/. Each of the 16 detection boxes contains 3 broadband interference filters set at wavelengths of 850, 950 and 1000 nm. This provides a means of checking the λ^{-2} scaling of bremsstrahlung intensity and gives an approximate measure of the absence of line radiation. Up to the silicon avalanche diodes used as detectors, the system is identical to that used for Thomson scattering. For the Z_{eff} measurements, however, a DC-coupled circuit with a bandwidth of 50 kHz is used. The sample rate is typically 200 Hz. Comparison of the Abel-inverted radiation with hydrogen bremsstrahlung determined from simultaneously measured n_e and T_e profiles results in Z_{eff} profiles from +20 cm to -38.5 cm with a spatial resolution of about 3 cm. Under some conditions comparisons have been made with radially averaged Z_{eff} values from plasma resistivity and from sawtooth analysis. The latter method is based on the electron power balance in ohmic discharges, in the plasma centre, during the period of recovery after the sawtooth crash /ref. 2/. In addition, Z_{eff} has been estimated from impurity densities derived by two methods. Firstly, absolutely measured VUV line intensities of the four dominant impurities (Fe, Cu, O, C) are compared with those calculated by a time dependent impurity transport code using measured n_e and T_e profiles.

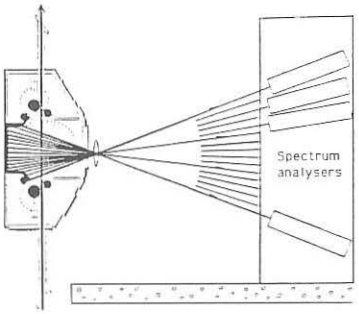

Fig. 1: Bremsstrahlung Z_{eff} setup

From this comparison an independent density profile is obtained for each impurity species, allowing its Z_{eff} contribution to be calculated. Secondly, the densities of the two light impurity species (O, C) can be also derived from charge exchange recombination spectroscopy (CXRS) resulting in an independent measurement of their Z_{eff} contribution. These spectroscopic Z_{eff} are generally less accurate than bremsstrahlung Z_{eff} but the resulting impurity densities yield considerable insight into the Z_{eff} behaviour reported in this paper.

Results and Discussion

Axial values of Z_{eff} as a function of n_e for steady state ohmic and co-NI heated discharges are shown in Figs. 2 and 3. Normally, Z_{eff} is found to decrease with increasing n_e, to be higher in D_+ than in H_+ plasmas, and higher in NI than in ohmic plasmas. The VUV Z_{eff} are in good agreement with the bremsstrahlung Z_{eff}, as are the sawtooth Z_{eff} for OH discharges in H_+. The CXRS Z_{eff} must be normalized to one point from the bremsstrahlung measurements because optical components of the CXRS diagnostic, inside the vacuum chamber, have been inaccessible to direct calibration. The CXRS Z_{eff} then show the same trends with n_e.

The above behaviour can be understood from the spectroscopic results. In ohmically and NI heated discharges O and C are the dominant light impurities with O giving the largest contribution to Z_{eff}. The VUV results for a transition from OH → co-NI heated plasma are shown in Fig. 4 for H_+ and Fig. 5 for D_+. The dominant heavy impurity in the H_+ discharge is Cu. It originates from the divertor plates and is more important at lower densities and in NI than in OH discharges. The densities of C and O (measured by VUV and CXRS) do not change strongly with n_e so it is this fact, together with the decrease of Cu, that explains the decrease in Z_{eff} with increasing n_e. Fe is unimportant in H_+ discharges due to carbonization, but gives a significant contribution to Z_{eff} in D_+ discharges where the walls were not carbonized (Figs. 3 and 5).

Particularly interesting are the Z_{eff} results obtained in three rather different scenarios in which improved energy confinement is found in ASDEX. These are OH discharges in D_+ with reduced gaspuff (Fig. 2) /Ref. 3/, pellet fuelled OH discharges (Fig. 6) /Ref. 4/, and counter-NI heated discharges (Fig. 7) /Ref. 5/.

In these cases there is a reversal of the trend of Z_{eff} decreasing with increasing n_e which shows that the improved energy confinement is accompanied by improved particle confinement. The strong accumulation of light impurities in counter NI discharges can be seen from the O^{8+} (Fig. 7) and C^{6+} densities. The relatively slow initial increase of $n_O{}^{8+}$ and $n_C{}^{6+}$ leads to a decrease of Z_{eff} as in the normal co-NI case. However, the impurity density increase is much steeper later on, so that Z_{eff} increases during the phase when the global energy confinement is also increasing. For counter-NI the neoclassical Z_{eff} is in good agreement with the bremsstrahlung Z_{eff} and this is also true for the OH pellet case (Fig. 6). In the improved confinement OH regime $Z_{eff}(r)$ shows slight peaking at the plasma centre at later times (Fig.8) but this is not seen in the pellet (Fig. 9) or counter-NI discharges.

Summary

The present measurements have shown a wide variety of behaviour of Z_{eff} in ASDEX plasmas and Z_{eff} values ranging from 1.2 to ~5 have been found. In particular, for three different improved energy confinement regimes, the Z_{eff} results indicate correspondingly improved particle confinement.

Ref. 1 H. Röhr, K.-H. Steuer et al., Nucl. Fusion 22 (1982), 1099
Ref. 2 A. Eberhagen, Internal Report IPP III/124, 1987
Ref. 3 E.R. Müller et al., this conference
Ref. 4 O. Gruber et al, this conference
Ref. 5 O. Gehre et al, Phys. Rev. Lett., to be published

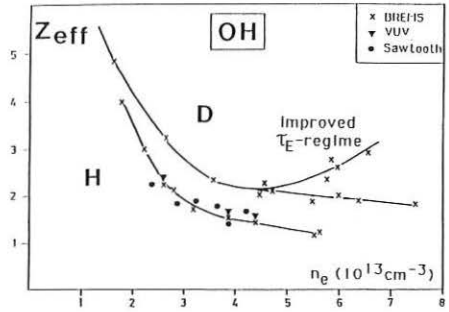

Fig. 2: Z_{eff} as a function of n_e for OH-plasmas in hydrogen (H) and deuterium (D).

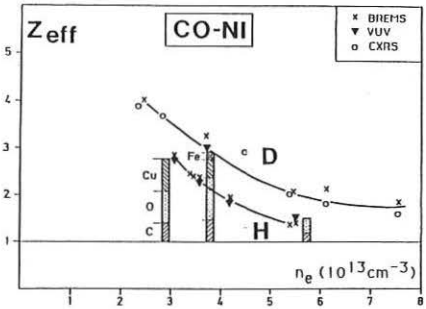

Fig. 3: Z_{eff} as a function of n_e for co-NI heated plasmas in H and D.

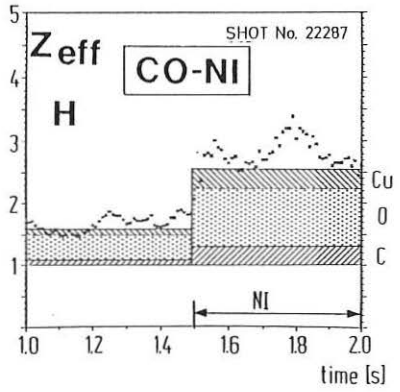

Fig. 4: bremsstrahlung Z_{eff} and the VUV imp. contributions during a transition from OH→co-NI in a hydrogen plasma.

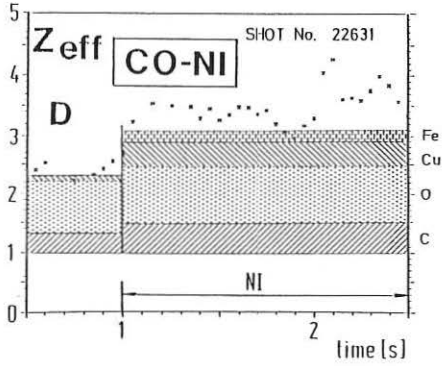

Fig. 5:
bremsstrahlung Z_{eff} and the VUV imp. contributions during a transition from OH→co-NI in a deuterium plasma.

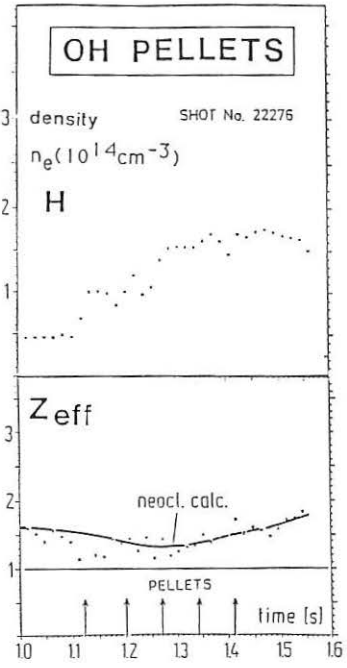

Fig. 6: Time dependence of n_e (above) and Z_{eff} (below) in a OH pellet refuelled discharge in hydrogen.

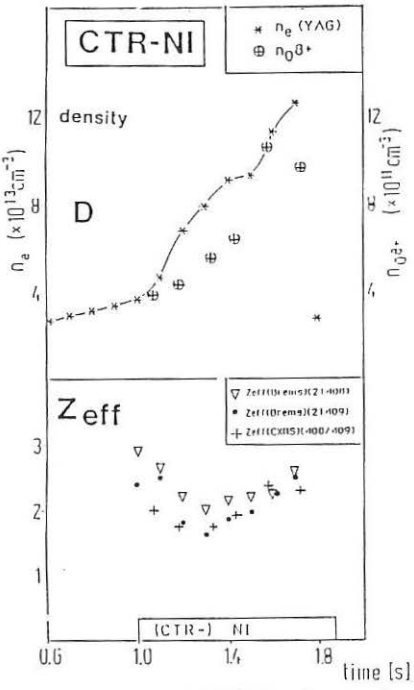

Fig. 7: Time dependence of n_e and n_O8+ (above) and Z_{eff} (below) in a counter NI heated discharge in deuterium.

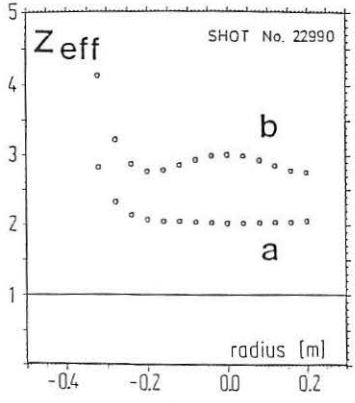

Fig.: 8: Radial profiles of Z_{eff} for OH discharges in deuterium. (a) "normal" regime, (b) improved confinement regime (n_{e0}=6.6 x $10^{13}cm^{-3}$, see Fig. 2).

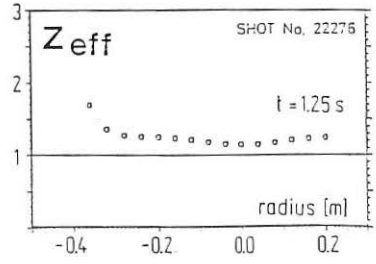

Fig.: 9: Radial profile of Z_{eff} for a pellet fuelled OH discharge in H (see Fig. 6).